



Boundary layer at
Dome C during
summer

H. Gallée et al.

This discussion paper is/has been under review for the journal Atmospheric Chemistry and Physics (ACP). Please refer to the corresponding final paper in ACP if available.

Characterization of the boundary layer at Dome C (East Antarctica) during the OPALE summer campaign

H. Gallée¹, S. Preunkert¹, S. Argentini², M. M. Frey³, C. Genthon¹, B. Jourdain¹, I. Pietroni², G. Casasanta², H. Barral¹, E. Vignon¹, and M. Legrand¹

¹CNRS/UJF – Grenoble 1, Laboratoire de Glaciologie et Géophysique de l'Environnement (LGGE), France

²Istituto di Scienze dell' Atmosfera e del Clima (ISAC) – CNR, Italy

³British Antarctic Survey, Natural Environment Research Council, Cambridge, UK

Received: 20 October 2014 – Accepted: 1 December 2014 – Published: 23 December 2014

Correspondence to: H. Gallée (gallee@lgge.obs.ujf-grenoble.fr)

Published by Copernicus Publications on behalf of the European Geosciences Union.

Title Page

Abstract

Introduction

Conclusions

References

Tables

Figures



Back

Close

Full Screen / Esc

Printer-friendly Version

Interactive Discussion



Abstract

The regional climate model MAR was run for the region of Dome C located on the East Antarctic plateau, during Antarctic summer 2011–2012, in order to refine our understanding of meteorological conditions during the OPALE observation campaign. A very high vertical resolution is set up in the lower troposphere, with a grid spacing of roughly 2 m. Comparisons are made with observed temperatures and winds near the surface and from a 45 m high tower as well as sodar and radiation data. MAR is generally in very good agreement with the observations but sometimes underestimates cloud formation, leading to an underestimation of the simulated downward long-wave radiation. Absorbed short-wave radiation may also be slightly overestimated due to an underestimation of the snow albedo and this influences the surface energy budget and atmospheric turbulence. Nevertheless the model provides sufficiently reliable information that represent key parameters when discussing the representativeness of chemical measurements made nearby the ground surface during field campaigns conducted at the Concordia site located at Dome C (3233 m a.s.l.).

1 Introduction

The aim of this paper is to validate MAR (Modèle Atmosphérique Régional) simulations covering the OPALE summer campaign, which took place at Concordia during austral summer 2011–2012 (from late November 2011 to mid-January 2012), for use for the interpretation of the chemistry observations carried out during the campaign. It is intended in particular to characterize the behaviour and the vertical structure of the boundary layer circulation at Dome C during this period.

Such an approach has been already done over the antarctic plateau, but with a simpler vertical 1-d model, which has been evaluated from observations during summertime at Kohnen base, in Dronning Maud Land (Van As et al., 2006).

ACPD

14, 33089–33116, 2014

Boundary layer at Dome C during summer

H. Gallée et al.

Title Page

Abstract

Introduction

Conclusions

References

Tables

Figures



Back

Close

Full Screen / Esc

Printer-friendly Version

Interactive Discussion



**Boundary layer at
Dome C during
summer**H. Gallée et al.

[Title Page](#)[Abstract](#)[Introduction](#)[Conclusions](#)[References](#)[Tables](#)[Figures](#)[Back](#)[Close](#)[Full Screen / Esc](#)[Printer-friendly Version](#)[Interactive Discussion](#)

Dome C is an area where observation and modelling of the boundary layer has already been performed due to its particular location. Furthermore due to an already available set of observations, Dome C was recently selected as the test site for the next Gewex Atmospheric Boundary Layer Studies (GABLS4) model intercomparison (see <http://www.cnrm.meteo.fr/aladin/meshtml/GABLS4/GABLS4.html>). Indeed, despite the harsh environment of Antarctica it is well supplied by logistics for many reasons. It is a dome on the East Antarctic plateau and has been chosen in the framework of the EPICA project for drilling the ice core with the longest climate chronology ever recorded, allowing to study the climate of the last eight glacial cycles (EPICA community members, 2004). The EPICA project initiated extensive meteorological observations at Dome C, in order to establish firmly among others the relationship between Dome C climate and global climate. So the set-up of a regional model at the Dome C drilling site able (i) to assimilate large scale meteorological conditions and (ii) to simulate local atmospheric conditions may be helpful in establishing this relationship. The good management of logistics between the Concordia station and the Antarctic coast (Terre Adélie) and the low optical turbulence at Dome C also promoted the site for astronomical observations (see e.g., Swain and Gallée, 2006; Sadibekova et al., 2006). The main characteristic of meteorological conditions at Dome C is that turbulent conditions in the low troposphere are effective in a rather shallow layer only, especially during night-time (Pietroni et al., 2014). Sodar measurement and sonic anemometer measurements were done at the Concordia station to monitor the turbulent structure of the planetary boundary layer (PBL) in connection with the temperature inversion and estimate the PBL height in the frame of the ABLCLIMAT (Atmospheric Boundary Layer Climate) project (Argentini et al., 2013).

The 45 m high tower built up at Concordia is also a very useful tool for observing such conditions (Genthon et al., 2010, 2013). Short-term meteorological simulations have already been done over Dome C with a coupled atmosphere-snow model, focusing on the behaviour of the snow model (Brun et al., 2011). Long term simulations (i.e., without any reinitialisation of meteorological variables) of the Antarctic climate have also

**Boundary layer at
Dome C during
summer**

H. Gallée et al.

[Title Page](#)[Abstract](#)[Introduction](#)[Conclusions](#)[References](#)[Tables](#)[Figures](#)[Back](#)[Close](#)[Full Screen / Esc](#)[Printer-friendly Version](#)[Interactive Discussion](#)

been done, with a focus on their behaviour at Dome C. Swain and Gallée (2006) and Lascaux et al. (2011) used respectively the limited area models MAR and Meso-NH to compare the optical properties of the atmosphere at Dome C with those of other potential Antarctic sites for astronomical observations using a large telescope. Gallée and Gorodetskaya (2010) validated MAR for winter conditions, stressing on the difficulty to accurately simulate the downward long-wave radiation and proposing to include the influence of small airborne snow particles in the parametrization of the radiation transfer. MAR has also been used for providing information on the atmospheric turbulence at Dome C in summer, which appears to very significantly control the vertical distribution and concentrations of numerous atmospheric chemical species (Legrand et al., 2009; Kerbrat et al., 2012; Dommergue et al., 2012; Frey et al., 2013). Finally two years of observations at the Dome C tower were used to compare a long-term simulation of MAR with ECMWF analyses, showing the interest to represent the atmosphere with a fine vertical resolution (Genthon et al., 2013). Here we go a step further by validating the model for summer conditions in the frame of the OPALE campaign which took place during Austral summer 2011–2012.

The main objective of the paper is to provide tools from a meteorological point of view for future campaign dedicated to document the chemical composition of the Antarctic boundary layer of the East Antarctic plateau as well as for interpreting data gained during the OPALE campaigns as detailed in companion papers (see Legrand et al., 2014; Kukui et al., 2014; Frey et al., 2014, and Preunkert et al., 2014). More precisely atmospheric turbulence plays an important role in the evolution of NO_x , HONO, HCHO, or H_2O_2 emitted by the snow pack. Key parameters are surface turbulent fluxes and the height of the boundary layer, which is determined by vertical turbulent diffusion. These parameters are used in companion papers to determine the contribution of turbulence to the concentration of key atmospheric species emitted from the surface, driving the oxidant budget in the low troposphere at Dome C. Other parameters like cloud cover and wind direction are also considered. For example situations with an overcast sky

were not considered nor situations for which the wind direction is from Concordia station, since the air is then contaminated by pollutants emitted by the station.

The remaining of the paper is divided in 4 parts. The experimental set-up and the main characteristics of the MAR model are described in Sects. 2 and 3. The fourth section is dedicated to the evaluation of the model, looking in particular to the consequences of the simulated radiative transfer on the surface atmospheric budget and atmospheric turbulence.

2 Meteorological observations

2.1 ISAC (Istituto di Scienze dell' Atmosfera e del Clima)

One-year in situ turbulence and radiation measurements, as well as SL-sodar observations, were carried out at the Concordia station from December 2011 up to December 2012 in the frame of the *ABLCLIMAT (Atmospheric Boundary Layer Climate)* project (Argentini et al., 2013).

The SL-sodar (Argentini et al., 2011) is an improved version of the sodar described by Argentini and Pietroni (2010), with the possibility of zooming within the atmospheric surface-layer thermal turbulent structure. With the SL-sodar, the PBL height h is estimated following Casasanta et al. (2014). During convective conditions h was determined as the height above the zone of weak backscattered intensity of the acoustic waves emitted by the sodar. Under stable conditions, h was retrieved either from the minimum of the first derivative of the backscattered signal, either from its maximum curvature.

Measurements of turbulence are made with a Metek USA-1, a three-axes sonic thermo-anemometer (sampling frequency of 10 Hz) installed on a 3.5 m mast. The heat and momentum fluxes are estimated using the eddy covariance method. The longwave and shortwave radiation components (up and down) were measured using Kipp and Zonen CNR1 pyrgeometers and pyranometers installed 1.5 m above the snow surface.

2.2 LGGE (Laboratoire de Glaciologie et de Géophysique de l'Environnement)

Meteorological profiling is carried out along a 45 m tower at Dome C since 2008 (Genthon et al., 2010). Wind, temperature and moisture are monitored at six levels from the near surface (3.3 m) to near the top of the tower (41.9 m). The instruments occasionally fail due to the extreme weather conditions at Dome C (extreme low temperatures, frost deposition), however the record is almost continuous since 2009 and the instruments perform generally well in summer (Genthon et al., 2013). Genthon et al. (2011) have demonstrated that a warm bias affects temperature measurements in Antarctica in cases of weak winds if conventional passively (wind) ventilated radiation shields are used to protect solid state thermometers (e.g. the ubiquitously used platinum thermistors) from solar radiation. At Dome C, only the temperature measurements on the tower are made in aspirated shield and bias free. Further details of the profiling set up, instrumentation and results obtained so far can be found in Genthon et al. (2010, 2013).

2.3 BAS (British Antarctic Survey)

Measurements of turbulence are made with a Metek USA-1, a three-axes sonic thermoanemometer (sampling frequency of 25 Hz) mounted on a mast 4 m above the snow surface. The mast was co-located with OPALE detectors of chemical trace gas species in the clean-air sector at about 1.2 km distance from the 45 m meteorology tower (map in Frey et al., 2013). Atmospheric boundary layer parameters such as friction velocity u_* and Monin–Obukhov Length were computed from the three-dimensional wind components (u , v , w) and temperature (Frey et al., 2014, this issue). Processing in 10 min blocks included temperature cross-wind correction and a double coordinate rotation to force mean w to zero (Kaimal and Finnigan, 1994; Van Dijk et al., 2006).

Boundary layer at Dome C during summer

H. Gallée et al.

[Title Page](#)[Abstract](#)[Introduction](#)[Conclusions](#)[References](#)[Tables](#)[Figures](#)[Back](#)[Close](#)[Full Screen / Esc](#)[Printer-friendly Version](#)[Interactive Discussion](#)

3 Description of MAR

An overview of the regional climate model MAR is given here, focused on the description of the turbulence scheme. A more complete description can be found in Gallée and Schayes (1994), Gallée (1995) and Gallée et al. (2013).

MAR atmospheric dynamics are based on the hydrostatic approximation of the primitive equations. This approximation is correct when the vertical extent of the circulation (here the drainage flow) remains much smaller than the size of the grid (here 20 km). Nevertheless, it should be noted that non-hydrostatic processes may be responsible for a weak deceleration of the katabatic flow (Cassano and Parish, 2000). The vertical coordinate is the normalized pressure, with the model top situated at the 1 Pa pressure level. Parametrization of turbulence in the surface boundary layer (SBL) is based on the Monin–Obukhov similarity theory and is completed by taking into account the stabilization effect by the blowing snow flux, as in Gallée et al. (2001) (see also Wamser and Lykossov, 1995). Turbulence above the SBL is parameterized using the local $E-\varepsilon$ model, consisting in two prognostic equations for turbulent kinetic energy and its dissipation. The prognostic equation of dissipation allows to relate the mixing length to local sources of turbulence and not only to the surface. The $E-\varepsilon$ model used here has been adapted to stable conditions by Duynkerke (1988) and revised by Bintanja (2000), who included a parametrization of the turbulent transport of snow particles that is consistent with classical parametrizations of their sedimentation velocity. The influence of changes in the water phase on turbulence is included following Duynkerke and Driedonks (1987). The relationship between the turbulent diffusion coefficient for momentum and scalars (Prandtl number) is dependant on the Richardson number, according to Sukorianski et al. (2005).

Prognostic equations are used to describe five water related parameters, as in Gallée (1995): specific humidity, cloud droplets and ice crystals, raindrops and snow particles. A sixth equation has been added describing the number of ice crystals, and the influence of hydrometeors on air specific mass is included in the model as in Gallée

Boundary layer at Dome C during summer

H. Gallée et al.

Title Page

Abstract

Introduction

Conclusions

References

Tables

Figures



Back

Close

Full Screen / Esc

Printer-friendly Version

Interactive Discussion



et al. (2001). This allows us to account for the influence of the weight of eroded particles on atmospheric flow dynamics by representing the pressure gradient force as a function of air density rather than of potential temperature only.

The radiative transfer through the atmosphere is parameterized following Morcrette (2002) and is the same as that used in ERA-40 re-analyses. As blowing snow particles are small (Walden et al., 2003), they may have an impact on the radiative transfer. Influence of snow particles on atmospheric optical depth is included in the MAR model (Gallée and Gorodetskaya, 2010).

Surface processes are modelled using the “soil-ice-snow-vegetation-atmosphere transfer” scheme (SISVAT, De Ridder and Gallée, 1998; Gallée et al., 2001; Lefebvre et al., 2005; Fettweis et al., 2005). In particular, the snow surface albedo depends on the snow properties (dendricity, sphericity and size of the snow particles). The influence of snow erosion/deposition on surface roughness (z_0) is taken into account by allowing the aerodynamic roughness length to increase linearly as a function of the wind speed at 10 m above the ground level (a.g.l.) (V_{10}), when $V_{10} > 6 \text{ m s}^{-1}$. The time scale for sastrugi formation is assumed to be half a day, as suggested by Andreas (1995), and the asymptotic value of the surface roughness length z_0 may increase linearly as a function of the wind speed V ($z_{0,\text{lim}} = 1.5 \text{ mm}$ for $V = 10 \text{ m s}^{-1}$; note that the friction velocity corresponding to $V = 10 \text{ m s}^{-1}$ is generally slightly greater than 0.5 m s^{-1}). z_0 is allowed to decrease when precipitation occurs with no erosion of the snow by the wind. Indeed the newly deposited snow progressively buries the sastrugi. Andreas et al. (2005, their Fig. 1) found values of z_0 ranging between approximately 10^{-4} and 100 mm, for friction velocities no greater than 0.6 m s^{-1} . Also observations by King and Anderson (1994) at Halley with similar snow properties as at Dome C, being compacted, sintered firn with some sastrugi revealed z_0 value of $(5.6 \pm 0.6) \times 10^{-5} \text{ m}$. The scatter is very high and is explained by the high dependency of z_0 on sastrugi history. Our parametrization includes that effect in a simple way, and is calibrated to obtain the best simulation of the wind speed.

Boundary layer at Dome C during summer

H. Gallée et al.

Title Page

Abstract

Introduction

Conclusions

References

Tables

Figures



Back

Close

Full Screen / Esc

Printer-friendly Version

Interactive Discussion



4 Evaluation of MAR

We here used the 3-D version in order to take into account a possible influence of the inversion wind circulation over the Dome C area, as suggested by Pietroni et al. (2014). The MAR domain is represented in Fig. 1. The horizontal grid size is 20 km and the vertical discretization in the lower troposphere is 2 m, with 60 levels. The vertical resolution decreases with altitude above 32 m.a.g.l., reaching 50 m at 300 m.a.g.l. and 400 m at 3000 m.a.g.l. A simulation with a vertical grid spacing of 1 m has also been done, without any significant change. The results obtained with this 1 m vertical grid have been used to discuss the behaviour of different chemical species, in particular their diurnal cycles, as presented in other papers of this issue (Legrand et al., 2014; Kukui et al., 2014; Frey et al., 2014; and Preunkert et al., 2014).

The MAR model is nested into the European re-analyses ERA-Interim (Dee et al., 2011). A relaxation zone of 5 grid points is prescribed at each lateral boundary (Marbaix et al., 2003) and model variables are nudged to the re-analysed variables in the upper 6 layers, i.e., above 13 km a.g.l. at Dome C. As the OPALE campaign took place from early December 2011 until mid January 2012, the MAR simulations were covering 3 months (from 1 November 2011 until 31 January 2012). The model variables are assumed to adapt to Dome C conditions during the first simulated month (i.e., November 2011). The snow pack is initialized with a density of 300 kg m^{-3} and assuming the presence of small grains, giving a slightly too low initial albedo (close to 0.79 at noon), while its value is in the range of 0.80–0.81 (Brun et al., 2011). Our analysis focuses on the period between 12 December 2011 and 14 January 2012, when most of the OPALE observations were made.

A problem already encountered when running the model over Adélie Land (East Antarctica) was an underestimation of the cloud cover (but not always) and the subsequent underestimation (overestimation) of the downward long-wave (short-wave) radiation. An underestimation (overestimation) of air temperatures near the surface during night-time (day-time) results (Gallée et al., 2013). Note however that the underestima-

Boundary layer at Dome C during summer

H. Gallée et al.

Title Page

Abstract

Introduction

Conclusions

References

Tables

Figures



Back

Close

Full Screen / Esc

Printer-friendly Version

Interactive Discussion



tion of the cloud cover is generally not critical since situations with an overcast sky are discarded when interpreting atmospheric chemistry measurements.

Here we consider the possibility that this problem could also occur in the MAR simulations at Dome C. We note first that MAR generally underestimates both the short-wave and long-wave downward radiations, with a bias of about 24.3 and 20.8 W m⁻², respectively (Table 1). The influence of the former on the surface energy budget is nevertheless less important than that of the latter, because of the high value of the snow albedo.

Let us now examine the downward long-wave radiation and the air temperature near the surface (Fig. 2). Both observation and simulation exhibit rapid variations in the long-wave downward radiation (LWD) (Fig. 2a). The correlation coefficient between the simulated LWD and cloud optical thickness is 0.79 for a 10 min time interval between each value of these variables, suggesting that cloud cover changes are responsible for most of these variations.

Figure 2b compares the daily averaged bias (simulation minus observation) in the long-wave downward radiations (LWD) and air temperatures near the surface at Dome C. The former is generally underestimated, leading to the underestimation of the latter (see also Table 1). A significant correlation may be seen between both biases, even when the temperature bias may be positive while the long-wave downward radiation bias remains negative. But the latter bias is partially compensated by a slight positive bias in the absorbed solar radiation (Table 1), probably because of an underestimation of MAR snow surface albedo.

In contrast, the bias in the absorbed solar radiation may become negative, for example on 10 and 11 January 2012, when the bias in the long-wave downward radiation is almost zero and significant snowfall is simulated. The positive temperature bias on 31 December 2011 is probably due to an overestimation of the long-wave downward radiation by MAR.

Thus, MAR underestimates cloud cover at Dome C, but not always. Note that this is also the case along the Adélie Land Coast (see Gallée et al., 2013). This underesti-

**Boundary layer at
Dome C during
summer**

H. Gallée et al.

Title Page

Abstract

Introduction

Conclusions

References

Tables

Figures



Back

Close

Full Screen / Esc

Printer-friendly Version

Interactive Discussion



mation is responsible for an underestimation of the downward long-wave radiation. As long-wave downward radiation plays a key role in the surface energy budget and the subsequent behaviour of turbulence near the surface, this point will be considered in the remaining of the paper.

Next we look at the main meteorological variables (wind speed, temperature) near the surface. The performances of the simulated temperature and wind speed are summarized in Table 1 by the correlation between simulation and observation, the bias (simulation minus observation), the root mean square error (RMSE) and the efficiency statistical test (E) proposed by Nash and Sutcliffe (1970):

$$E = 1 - \text{RMSE}^2 / s^2 \quad (1)$$

where s and RMSE are respectively the SD of the observations and the root-mean-square error of the simulated variable. Note that $\text{RMSE} = 0$ implies $E = 1$. An efficiency index greater than 0 also means that comparing the simulated variable with the corresponding observation provides a lower RMSE than that obtained when comparing it with its time average. A negative efficiency index means that the RMSE is higher than the SD of the observations. This then suggests that a detailed model would not improve the results when compared to a simpler model providing an estimation of the variable averaged over the time period concerned.

It is found that the efficiency statistical test for temperature and wind speed is no smaller than 0.677 for all comparisons (Table 1), giving us confidence into the model.

We here examine in more details wind speed and temperature. The comparison between simulated and observed wind speed 3 m above the surface is shown in Fig. 3a. The agreement is good, as also quantified by the efficiency (0.737, Table 1). The agreement between the simulated and observed wind direction is also excellent, as it can be seen by eye (Fig. 3b). This behaviour indicates that the model is able to capture the atmospheric circulation at Dome C at the synoptic scale and is able to simulate the local circulation. Both observation and simulation reveal two preferential wind directions, one from the plateau (southerly winds) and the other from the ocean (northerly winds).

Boundary layer at Dome C during summer

H. Gallée et al.

Title Page

Abstract

Introduction

Conclusions

References

Tables

Figures



Back

Close

Full Screen / Esc

Printer-friendly Version

Interactive Discussion



**Boundary layer at
Dome C during
summer**

H. Gallée et al.

Title Page

Abstract

Introduction

Conclusions

References

Tables

Figures



Back

Close

Full Screen / Esc

Printer-friendly Version

Interactive Discussion



A well-marked diurnal cycle is generally found in the wind speed but does not exist in the wind direction. Wind speed peaks during the afternoon, when turbulent fluxes in the well mixed layer are able to transport momentum downwards more efficiently. Wind speed is also generally stronger and may be larger than 6 m s^{-1} in case of wind blowing from the North, except on 5–7 January 2012, when wind was blowing from the South. The behaviour of the simulated air temperature is also good (Fig. 3c), although the diurnal cycle is generally more marked than observed, especially for night-time (not shown for tower and BAS observations). The largest differences are found when comparing with the observations at the tower. Tower observations are made in aspirated shields which have been demonstrated to avoid large warm biases with the most often used passively ventilated shields in cases of weak winds (Gentson et al., 2011). These are the only measurements of temperature at Dome C carried out in aspirated shields, and thus except for sonic measurements the only unaffected by radiations biases.

Finally the good behaviour of the simulated friction velocity (Fig. 3d) suggests that MAR simulates surface meteorological variables for the right reasons. From the previous analysis we have some confidence on the behaviour of the model in the surface boundary layer at Dome C during the OPALE observation period, but some discrepancies with the observations are found.

4.1 Period between 26 and 28 December 2011

We here focus on the period between 26 and 28 December 2011, which is a period of intensive observations of chemical species. This period is characterized by winds coming from the high East Antarctic plateau and by an absence of clouds except between 09:00 and 15:00 LT on 26 December and between 04:00 and 11:00 LT on 27 December, when the downward long-wave flux (LWD) is relatively large in the observations. Unfortunately MAR underestimates LWD at those times (see Fig. 2a).

We show in Fig. 4a the behaviour of the simulated temperature and wind speed at the tower, between 3.3 and 41.9 m a.g.l. The simulation exhibits a marked diurnal cycle, with a strong temperature inversion during night-time and a well mixed layer during

**Boundary layer at
Dome C during
summer**

H. Gallée et al.

[Title Page](#)[Abstract](#)[Introduction](#)[Conclusions](#)[References](#)[Tables](#)[Figures](#)[Back](#)[Close](#)[Full Screen / Esc](#)[Printer-friendly Version](#)[Interactive Discussion](#)

day-time. During night-time a close link exists between the vertical temperature gradient and the vertical wind speed gradient. The latter is the highest where vertical stability associated with temperature increasing strongly with height is the largest. Such a behaviour is often referred to as a decoupling between the cold air near the surface and the warmer air above. This decoupling is also found in a change of the wind direction just above the turbulent layer. Convective mixing during day-time precludes this behaviour, and the vertical gradients of both temperature and wind speed are much smaller. Night-time decoupling and day-time mixing are also found in the observations, but with some differences due to the presence of clouds that the model was not able to simulate.

It is seen in Fig. 4b that the model indicates a warm bias on 26 December 2011 until 18:00 LT, except below 10 m a.g.l. until 06:00 LT. Probably the absence of simulated clouds is responsible for an overestimation of the surface absorbed solar radiation and the subsequent heating of the surface. The heat excess is then transferred to the atmosphere through turbulent mixing. Note that the marked overestimation by the model of the simulated absorbed solar radiation and air temperature are not repeated on 27 and 28 December 2011. Nevertheless temperature maxima are overestimated by roughly 1 to 1.5 °C, both at the surface (not shown) and above.

Air temperatures on 27 and 28 December in the morning are underestimated in the MAR simulations, especially on 28 December. An underestimation of about 10 W m⁻² or more is also found in the downward long-wave radiation (LWD), even in the absence of clouds (Fig. 2a). Simulated and observed turbulent fluxes are compared in Fig. 5. The simulated friction velocity is slightly underestimated by the MAR model during night-time, especially on 28 December, while the simulated downward turbulent heat flux is comparable to the observations or slightly overestimated. Possibly the simulated surface turbulent heat flux would have been larger if the friction velocity had not been underestimated by the model at that time. Furthermore, the slight overestimation of the air temperature above 10–15 m a.g.l. (Fig. 4b) could also result from an insufficient turbulent mixing during night-time, explaining also partly the underestimation of the air

**Boundary layer at
Dome C during
summer**

H. Gallée et al.

Title Page

Abstract

Introduction

Conclusions

References

Tables

Figures



Back

Close

Full Screen / Esc

Printer-friendly Version

Interactive Discussion



temperature near the surface. Thus it could be argued that an initial underestimation of the air temperature near the surface may be responsible for an increased vertical stability, reinforcing the decoupling between the lower troposphere and the atmosphere above, but a possible leading role of an underestimation of LWD must be firmly established.

From Fig. 5 it is also found that MAR underestimates the upward turbulent heat flux during day-time, when observed clouds were not simulated (on 26 December around noon and on 27 December in the morning) while it overestimates it when clouds are not present nor in the observation nor in the simulation (on 27 and 28 December during day-time). No definite explanation was found about the underestimation but the overestimation may be related to a too large heating of the surface and an overestimation of the air temperature by the model (see Fig. 4b), suggesting that the overestimation of air temperature at that time is driven by the surface.

Biases in the simulated wind speed could be linked to biases in the simulated air temperature, but not always. An example of such a link in Fig. 4b is a positive wind speed bias simulated between 15:00 and 18:00 LT on 26 December 2011. It could be associated with the positive bias in the downward short-wave radiation. At that time the overestimated turbulent mixing could lead to an overestimated height of the turbulent layer and an overestimated downward transfer of momentum. Indeed simulated wind speeds are larger at the upper levels of the tower at that time (Fig. 4a) and the model overestimates the height of the well-mixed layer (Fig. 6). The bias in the wind speed decreases after 18:00 LT especially below 25 m a.g.l. This is due to an increasing stability near the surface and the subsequent decoupling between the layer of air near the surface and the layer above. Wind speeds are still overestimated above up to the highest level of the tower, possibly because of an overestimated vertical extent of the residual mixed layer at that time.

Observations suggest the onset of a nocturnal jet after 18:00 LT, with a maximum of 7 ms^{-1} around 20 m a.g.l. around 22:00 LT. MAR also simulates a nocturnal jet at that time but around 140 m a.g.l., and slightly stronger (8 ms^{-1}) (not shown). This oc-

Boundary layer at Dome C during summer

H. Gallée et al.

[Title Page](#)[Abstract](#)[Introduction](#)[Conclusions](#)[References](#)[Tables](#)[Figures](#)[Back](#)[Close](#)[Full Screen / Esc](#)[Printer-friendly Version](#)[Interactive Discussion](#)

currence is consistent with a higher extent of the residual layer and may be the consequence of the sudden shut down of the turbulent mixing at 18:00 LT at that level in the model (not shown), while the pressure gradient force (PGF) still contributes to an increase of the wind speed after that time. Such an evolution is typical for a convective mixed layer at the end of day-time, and is also observed at lower latitudes. The contribution of PGF to the acceleration of the wind starts to decrease after 20:30 LT. In fact nocturnal low level jets have been so frequent during OPALE that the analysis of this process deserves some attention. This topic will be addressed in a companion note by analysing a case study which is well simulated by the model (Gallée et al., 2014, this issue).

A temperature positive bias seems also to occur on 06:00 LT on 27 December 2011 above 25 m a.g.l. Its behaviour is similar to that of 26 December and it occurs also in conjunction with an underestimation of the cloud cover by the model and an earlier deepening of the well-mixed layer, but it is less marked.

5 Discussion and conclusion

MAR has been set up over a domain covering Dome C during the OPALE campaign. The size of the domain is much smaller than the internal radius of deformation. Such choice constrains the model solution in the free atmosphere by that of the host model (here the European re-analyses ERA-Interim) but, as already pointed out by Lefebvre et al. (2005), it allows it to develop its own solution in the boundary layer. The simulation is characterized by a positive efficiency of wind and temperature over Dome C, given us confidence in its behaviour. MAR underestimates the downward long-wave radiation, but not always. When it occurs this problem is probably caused by an underestimation of the cloud cover and may be one of the causes being responsible for an overestimation of the amplitude of the diurnal cycle of air temperatures by the model. Other possible causes are an underestimation of heat transfer in the snow pack and an amplification of the subsequent decoupling between the atmosphere and the surface initiated

**Boundary layer at
Dome C during
summer**

H. Gallée et al.

Title Page

Abstract

Introduction

Conclusions

References

Tables

Figures



Back

Close

Full Screen / Esc

Printer-friendly Version

Interactive Discussion



by the underestimated LWD and heat conduction. Indeed surface turbulent fluxes are well simulated, but discrepancies with the observations are found when the simulated downward long-wave flux is underestimated. On the other hand the simulated wind speed in the surface boundary layer is in good agreement with the observations. It may consequently be argued that the turbulence schemes used in MAR (Monin–Obukhov similarity theory and E- ε model) are valid for the OPALE period. The question of whether it remains valid, especially under stronger winter radiational cooling is still open.

Consequently model outputs and especially its turbulent characteristic are useful when interpreting the observations made in case of observed clear sky during OPALE. Indeed clear sky conditions, i.e. situations for which the model simulation is in excellent agreement with available observations, are more adequate when discussing measurements of species involved in photochemical processes. In particular the good behaviour of the simulated surface turbulent fluxes allows us to use the associated turbulent eddy diffusivity coefficient to evaluate the impact of turbulent transport on NO_x, HONO and HCHO emitted from snow. In addition the simulated boundary layer height indicates over which thickness of the atmosphere these chemical species are diluted. In brief, the use of such a model will allow us to optimize the experimental set-up for future campaign aiming to characterize the low troposphere chemistry at Dome C.

Acknowledgements. The OPALE project was funded by the ANR (Agence National de Recherche) contract ANR-09-BLAN-0226.

Most of the computations presented in this paper were performed using the Froggy platform of the CIMENT infrastructure (<https://ciment.ujf-grenoble.fr>), which is supported by the Rhône-Alpes region (GRANT CPER07_13 CIRA), the OSUG@2020 labex (reference ANR10 LABX56) and the Equip@Meso project (reference ANR-10-EQPX-29-01) of the programme Investissements d'Avenir supervised by the Agence Nationale pour la Recherche. This work was also granted access to the HPC resources of [TGCC/CINES/IDRIS] under the allocation 2014-1523 made by GENCI.

IPEV-CALVA, INSU-LEFE-CLAPA and OSUG GLACIOCLIM-CENACLAM projects are acknowledged for their support.

References

- Andreas, E. L.: Physically based model of the form drag associated with sastrugi, US Army Cold Regions Research and Engineering Laboratory, Hanover, NH, CRREL Report No CR 95-16, 12 pp., 1995.
- Argentini, S. and Pietroni, I.: An integrated observing system for boundary layer monitoring at Concordia Station, Antarctica, in: Integrated Ground-Based Observing Systems, edited by: Cimini, D., Marzano, F., and Visconti, G., Springer-Verlag, Berlin Heidelberg, 199–208, 2010.
- Argentini, S., Pietroni, I., Mastrantonio, G., Petenko, I., and Viola, A.: Use of a high-resolution sodar to study surface-layer turbulence at night, *Bound.-Lay. Meteorol.*, 143, 177–188, 2011.
- Argentini, S., Petenko, I., Viola, A., Mastrantonio, G., Pietroni, I., Casasanta, G., Aristidi, E., and Genthon, C.: The surface layer observed by a high-resolution sodar at DOME C, Antarctica, *Ann. Geophys.-Italy*, 56, 1–10, doi:10.4401/ag-6347, 2013.
- Bintanja, R.: Snowdrift suspension and atmospheric turbulence. Part I: Theoretical background and model description, *Bound.-Lay. Meteorol.*, 95, 343–368, 2000.
- Brun, E., Six, D., Picard, G., Vionnet, V., Arnaud, L., Bazile, E., Boone, A., Bouchard, A., Genthon, C., Guidard, V., Le Moigne, P., Rabier, F., and Seity, Y.: Snow/atmosphere coupled simulation at Dome C, Antarctica, *J. Glaciol.*, 52, 721–736, 2011.
- Casasanta, G., Pietroni, I., Petenko, I., and Argentini, S.: Observed and modelled convective mixing-layer height at Dome C, Antarctica, *Bound.-Lay. Meteorol.*, 151, 597–608, doi:10.1007/s10546-014-9907-5, 2014.
- Cassano, J. J. and Parish, T. R.: An analysis of the nonhydrostatic dynamics in numerically simulated Antarctic katabatic flows, *J. Atmos. Sci.*, 57, 891–898, 2000.
- Dee, D. P., Uppala, S. M., Simmons, A. J., Berrisford, P., Poli, P., Kobayashi, S., Andrae, U., Balmaseda, M. A., Balsamo, G., Bauer, P., Bechtold, P., Beljaars, A. C. M., van de Berg, L., Bidlot, J., Bormann, N., Delsol, C., Dragani, R., Fuentes, M., Geer, A. J., Haimberger, L., Healy, S. B., Hersbach, H., Hólm, E. V., Isaksen, L., Kållberg, P., Köhler, M., Matricardi, M., McNally, A. P., Monge-Sanz, B. M., Morcrette, J.-J., Park, B.-K., Peubey, C., de Rosnay, P., Tavolato, C., Thépaut, J.-N., and Vitart, F.: The ERA-Interim reanalysis: configuration and

**Boundary layer at
Dome C during
summer**H. Gallée et al.

[Title Page](#)[Abstract](#)[Introduction](#)[Conclusions](#)[References](#)[Tables](#)[Figures](#)[Back](#)[Close](#)[Full Screen / Esc](#)[Printer-friendly Version](#)[Interactive Discussion](#)

performance of the data assimilation system, Q. J. Roy. Meteor. Soc., 137, 553–597. doi:10.1002/qj.828, 2011.

De Ridder, K. and Gallée, H.: Land surface-induced regional climate change in southern Israel, J. Appl. Meteorol., 37, 1470–1485, doi:10.1175/1520-0450, 1998.

5 Dommergue, A., Barret, M., Courteaud, J., Cristofanelli, P., Ferrari, C. P., and Gallée, H.: Dynamic recycling of gaseous elemental mercury in the boundary layer of the Antarctic Plateau, Atmos. Chem. Phys., 12, 11027–11036, doi:10.5194/acp-12-11027-2012, 2012.

Duykerke, P. G.: Application of the E- ϵ turbulence closure model to the neutral and stable atmospheric boundary layer, J. Atmos. Sci., 45, 865–880, 1988.

10 Duykerke, P. G. and Driedonks, A. G. M.: A model for the turbulent structure of the stratocumulus-topped atmospheric boundary layer, J. Atmos. Sci., 44, 43–64, 1987.

EPICA community members: eight glacial cycles from an Antarctic ice core, Nature, 429, 623–628, 2004.

15 Fettweis, X., Gallée, H., Lefebvre, F., and Van Ypersele, J.: Greenland surface mass balance simulated by a regional climate model and comparison with satellite derived data in 1990–1991, Clim. Dynam., 24, 623–640. doi:10.1007/s00382-005-0010-y, 2005.

Frey, M. M., Brough, N., France, J. L., Anderson, P. S., Traulle, O., King, M. D., Jones, A. E., Wolff, E. W., and Savarino, J.: The diurnal variability of atmospheric nitrogen oxides (NO and NO₂) above the Antarctic Plateau driven by atmospheric stability and snow emissions, Atmos. Chem. Phys., 13, 3045–3062, doi:10.5194/acp-13-3045-2013, 2013.

20 Frey, M. M., Roscoe, H. K., Kukui, S., Savarino, J., France, J. L., King, M. D., Legrand, M., and Preunkert, S.: Atmospheric nitrogen oxides (NO and NO₂) at Dome C, East Antarctica, during the OPAL campaign, submitted, 2014.

Gallée, H.: Simulation of the mesocyclonic activity in the Ross Sea, Antarctica, Mon. Weather Rev., 123, 2051–2069, 1995.

25 Gallée, H. and Gorodetskaya, I.: Validation of a limited area model over Dome C, Antarctic Plateau, during winter, Clim. Dynam., 23, 61–72, doi:10.1007/s00382-008-0499-y, 2010.

Gallée, H. and Schayes, G.: Development of a three-dimensional meso-gamma primitive equations model, katabatic winds simulation in the area of Terra Nova Bay, Antarctica, Mon. Weather Rev., 122, 671–685, 1994.

30 Gallée, H., Guyomarc'h, G., and Brun, E.: Impact of snow drift on the Antarctic Ice Sheet surface mass balance. Possible sensitivity to snow surface properties, Bound.-Lay. Meteorol., 99, 1–19, 2001.

Boundary layer at Dome C during summer

H. Gallée et al.

Title Page

Abstract

Introduction

Conclusions

References

Tables

Figures



Back

Close

Full Screen / Esc

Printer-friendly Version

Interactive Discussion



Gallée, H., Trouvilliez, A., Agosta, C., Genthon, C., Favier, V., and Naaim-Bouvet, F.: Transport of snow by the wind: a comparison between observations made in Adélie Land, Antarctica, and simulations made with the regional climate model MAR, *Bound.-Lay. Meteorol.*, 146, 133–147; doi:10.1007/s10546-012-9764-z, 2013.

5 Genthon, C., Town, M. S., Six, D., Favier, V., Argentini, S., and Pellegrini, A.: Meteorological atmospheric boundary layer measurements and ECMWF analyses during summer at Dome C, Antarctica, *J. Geophys. Res.-Atmos.*, 115, D05104, doi:10.1029/2009JD012741, 2010.

Genthon, C., Six, D., Favier, V., Lazzara, M., and Keller, L.: Atmospheric temperature measurement biases on the Antarctic plateau, *J. Atmos. Ocean. Tech.*, 28, 1598–1605, doi:10.1175/JTECH-D-11-00095.1, 2011.

10 Genthon, C., Six, D., Gallée, H., Grigioni, P., and Pellegrini, P.: Two years of atmospheric boundary layer observations on a 45-m tower at Dome C on the Antarctic plateau, *J. Geophys. Res.-Atmos.*, 118, 3218–3232, doi:10.1002/jgrd.50128, 2013.

Kaimal, J. C., and J. J. Finnigan, *Atmospheric Boundary-Layer Flows: Their Structure and Measurement*, 289 pp., Oxford University Press, 1994.

15 Kerbrat, M., Legrand, M., Preunkert, S., Gallée, H., and Kleffmann, J.: Nitrous acid at Concordia on the East Antarctic Plateau and its transport to the coastal site of Dumont d'Urville, *J. Geophys. Res.*, 117, D08303, doi:10.1029/2011JD017149, 2012.

King, J. C. and Anderson, P. S.: Heat and water vapour fluxes and scalar roughness lengths over an Antarctic ice shelf, *Bound.-Lay. Meteorol.*, 69, 101–121, 1994.

20 Kukui, A., Legrand, M., Preunkert, S., Frey, M. M., Loisil, R., Gil Roca, J., Jourdain, B., King, M. D., France, J. L., and Ancellet, G.: Measurements of OH and RO₂ radicals at Dome C, East Antarctica, *Atmos. Chem. Phys.*, 14, 12373–12392, doi:10.5194/acp-14-12373-2014, 2014.

25 Lascaux, F., Masciadri, E., and Hagelin, S.: Mesoscale optical turbulence simulations above Dome C, Dome A and South Pole, *Mon. Not. R. Astron. Soc.*, 411, 693–704, doi:10.1111/j.1365-2966.2010.17709.x, 2011.

Lefebvre, F., Fettweis, X., Gallée, H., Van Ypersele, J., Marbaix, P., Greuell, W., and Calanca, P.: Evaluation of a high-resolution regional climate simulation over Greenland, *Clim. Dynam.*, 25, 99–116, doi:10.1007/s00382-005-0005-8, 2005.

30 Legrand, M., Preunkert, S., Jourdain, B., Gallée, H., Goutail, F., Weller, R., and Savarino, J.: Year round record of surface ozone at coastal (Dumont d'Urville) and inland (Concordia) sites in East Antarctica, *J. Geophys. Res.*, 114, D20306, doi:10.1029/2008JD011667, 2009.

**Boundary layer at
Dome C during
summer**

H. Gallée et al.

Title Page

Abstract

Introduction

Conclusions

References

Tables

Figures



Back

Close

Full Screen / Esc

Printer-friendly Version

Interactive Discussion



- Legrand, M., Preunkert, S., Frey, M., Bartels-Rausch, Th., Kukui, A., King, M. D., Savarino, J., Kerbrat, M., and Jourdain, B.: Large mixing ratios of atmospheric nitrous acid (HONO) at Concordia (East Antarctic Plateau) in summer: a strong source from surface snow?, *Atmos. Chem. Phys.*, 14, 9963–9976, doi:10.5194/acp-14-9963-2014, 2014.
- 5 Marbaix, P., Gallée, H., Brasseur, O., and Van Ypersele, J.: Lateral Boundary Conditions in regional climate models: a detailed study of the relaxation procedure, *Mon. Weather Rev.*, 131, 461–479, 2003.
- Morcrette, J.-J.: Assessment of the ECMWF model cloudiness and surface radiation fields at the ARM-SGP site, *Mon. Weather Rev.*, 130, 257–277, 2002.
- 10 Nash, J. E. and Sutcliffe, J. V.: River flow forecasting through conceptual models part I – A discussion of principles, *J. Hydrol.*, 10, 282–290, doi:10.1016/0022-1694(70)90255-6, 1970.
- Pietroni, I., Argentini, S., and Petenko, I.: One year of surface-based temperature inversions at Dome C, Antarctica, *Bound.-Lay. Meteorol.*, 150, 131–151, doi:10.1007/s10546-013-9861-7, 2014.
- 15 Preunkert, S., Legrand, M., Frey, M., Kukui, A., Savarino, J., Gallée, H., King, M., Jourdain, B., Vicars, W., and Helmig, D.: Formaldehyde (HCHO) in air, snow and interstitial air at Concordia (East Antarctic plateau) in summer, *Atmos. Chem. Phys. Discuss.*, 14, 32027–32070, doi:10.5194/acpd-14-32027-2014, 2014.
- Sadibekova, T., Fossat, E., Genthon, C., Krinner, G., Aristidi, E., Agabi, K., and Azouit, M.: 20 On the atmosphere for astronomers above Dome C, Antarctica, *Antarct. Sci.*, 18, 437–444, 2006.
- Sukoriansky, S., Galperin, P., and Veniamin, P.: Application of a new spectral theory on stably stratified turbulence to the atmospheric boundary layer over sea ice, *Bound.-Lay. Meteorol.*, 117, 231–257, 2005.
- 25 Swain, M. R. and Gallée, H.: Antarctic boundary layer seeing, *Astr. Soc. P.*, 118, 1190–1197, 2006.
- Van As, D., van den Broeke, M. R., and Helsen, M. M. Structure and dynamics of the summertime atmospheric boundary layer over the Antarctic plateau, I: Measurements and model validation, *J. Geophys. Res.*, 111, D007102, doi:10.1029/2005JD005948, 2006.
- 30 Van Dijk, A., Moen, A., and de Bruin, H.: The principles of surface flux physics: theory, practice and description of the ECPACK library, Internal report 2004/1, Meteorology and Air Quality Group, Wageningen University, Wageningen, the Netherlands, 2006.

Von Walden, P., Warren, S. G., and Tuttle, E.: Atmospheric ice crystals over the Antarctic Plateau in winter, *J. Appl. Meteorol.*, 42, 1391–1405, 2003.

Wamser, C. and Lykossov, V. N.: On the friction velocity during blowing snow, *Beitr. Phys. Atmosph.*, 68, 85–94, 1995.

**Boundary layer at
Dome C during
summer**

H. Gallée et al.

Title Page

Abstract

Introduction

Conclusions

References

Tables

Figures



Back

Close

Full Screen / Esc

Printer-friendly Version

Interactive Discussion



Boundary layer at Dome C during summer

H. Gallée et al.

Table 1. Correlation coefficient, bias, RMSE (root mean square error) and efficiency statistical test of the simulated short-wave downward radiation (SWD), the short-wave absorbed radiation by the surface (SWA), the long-wave downward radiation (LWD), the temperature and the wind speed when compared to the observations made by ISAC (Istituto di Scienze dell' Atmosfera e del Clima) (3rd and 4th column), by LGGE (Laboratoire de Glaciologie et de Géophysique de l'Environnement) (at the tower, 5th column) and by BAS (British Antarctic Survey) (6th column). Data were averaged over an interval of 30 min.

MAR		ISAC	ISAC 3 m	Tower 3 m	BAS 4 m
SWD	Bias	-24.3 W m^{-2}			
SWA	Bias	3.4 W m^{-2}			
LWD	Bias	-20.8 W m^{-2}			
Temperature	Corr. Coef.		0.981	0.912	0.973
	Bias		-0.387°C	-0.642°C	-0.551°C
	RMSE		2.408°C	2.778°C	2.735°C
	<i>E</i>		0.958	0.751	0.933
Wind Speed	Corr. Coeff.		0.865	0.872	0.856
	Bias		-0.227 ms^{-1}	-0.105 ms^{-1}	0.440 ms^{-1}
	RMSE		1.057 ms^{-1}	0.949 ms^{-1}	1.089 ms^{-1}
	<i>E</i>		0.737	0.752	0.677

[Title Page](#)
[Abstract](#)
[Introduction](#)
[Conclusions](#)
[References](#)
[Tables](#)
[Figures](#)
[◀](#)
[▶](#)
[◀](#)
[▶](#)
[Back](#)
[Close](#)
[Full Screen / Esc](#)
[Printer-friendly Version](#)
[Interactive Discussion](#)


**Boundary layer at
Dome C during
summer**

H. Gallée et al.

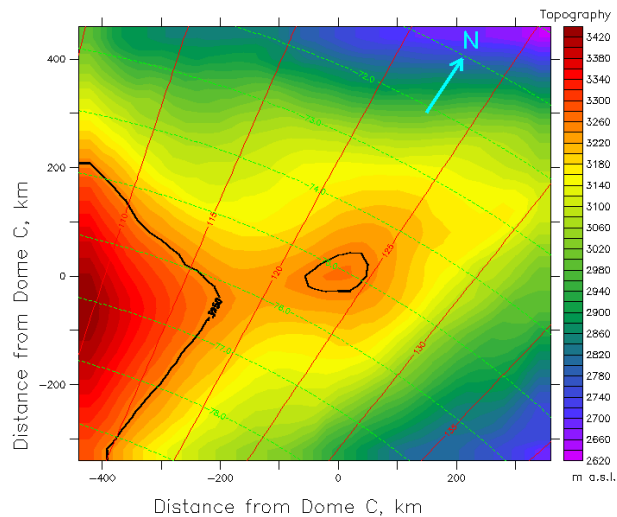


Figure 1. The MAR integration domain and topography. The solid line refers to the 3250 m isocontour.

[Title Page](#)[Abstract](#)[Introduction](#)[Conclusions](#)[References](#)[Tables](#)[Figures](#)[Back](#)[Close](#)[Full Screen / Esc](#)[Printer-friendly Version](#)[Interactive Discussion](#)

Boundary layer at Dome C during summer

H. Gallée et al.

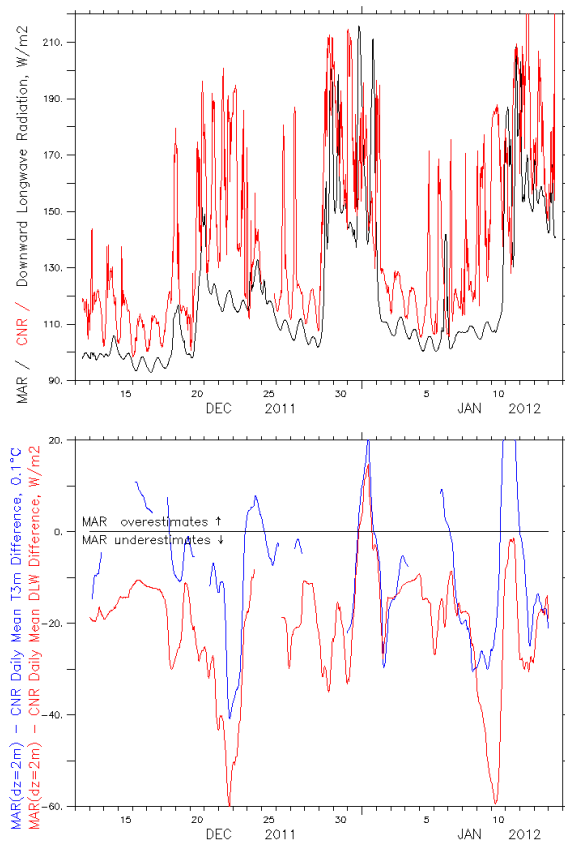


Figure 2. Top: long-wave downward radiation (LWD, W m^{-2}): simulation (dark line) and observation (red line). Data were averaged over an interval of 30 min. Bottom: comparison between the daily averaged LWD bias (red line) and air temperature bias (blue line, units: 0.1°C). Observations are those of the ISAC. MAR temperatures are averaged between 2 and 4 m a.g.l.. Gaps correspond to the absence of observations.

[Title Page](#)
[Abstract](#)
[Introduction](#)
[Conclusions](#)
[References](#)
[Tables](#)
[Figures](#)
[◀](#)
[▶](#)
[◀](#)
[▶](#)
[Back](#)
[Close](#)
[Full Screen / Esc](#)
[Printer-friendly Version](#)
[Interactive Discussion](#)


Boundary layer at
Dome C during
summer

H. Gallée et al.

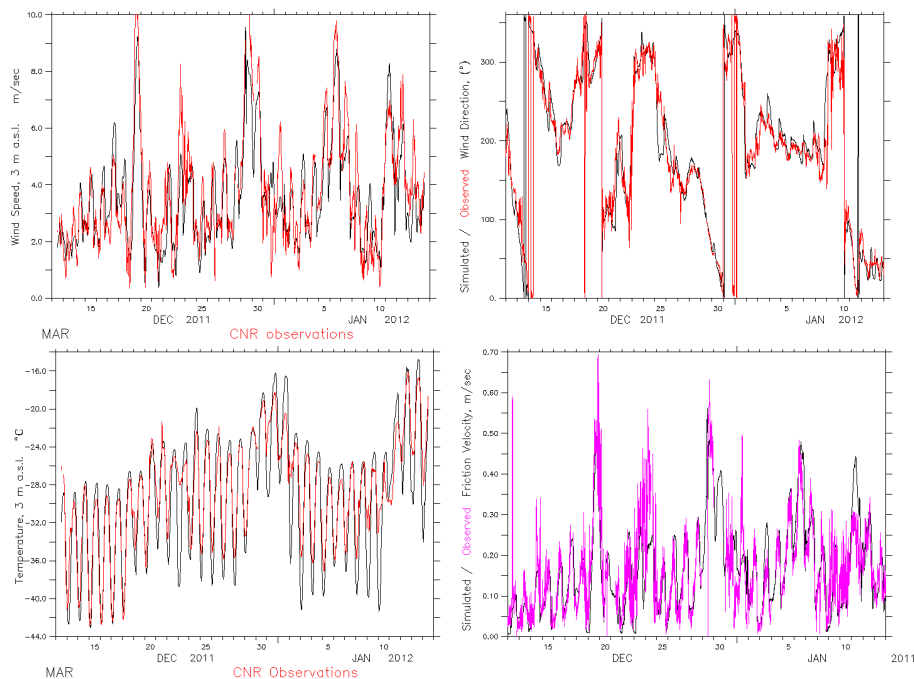


Figure 3. Simulation (dark line) of wind speed (top left), wind direction (top right), and air temperature (bottom left) at Dome C, 3 m a.s.l., compared with ISAC observations. Bottom right: simulation of friction velocity (dark line) compared with BAS observations (magenta line). Data were averaged over an interval of 30 min.

[Title Page](#)[Abstract](#)[Introduction](#)[Conclusions](#)[References](#)[Tables](#)[Figures](#)[◀](#)[▶](#)[◀](#)[▶](#)[Back](#)[Close](#)[Full Screen / Esc](#)[Printer-friendly Version](#)[Interactive Discussion](#)

Boundary layer at
Dome C during
summer

H. Gallée et al.

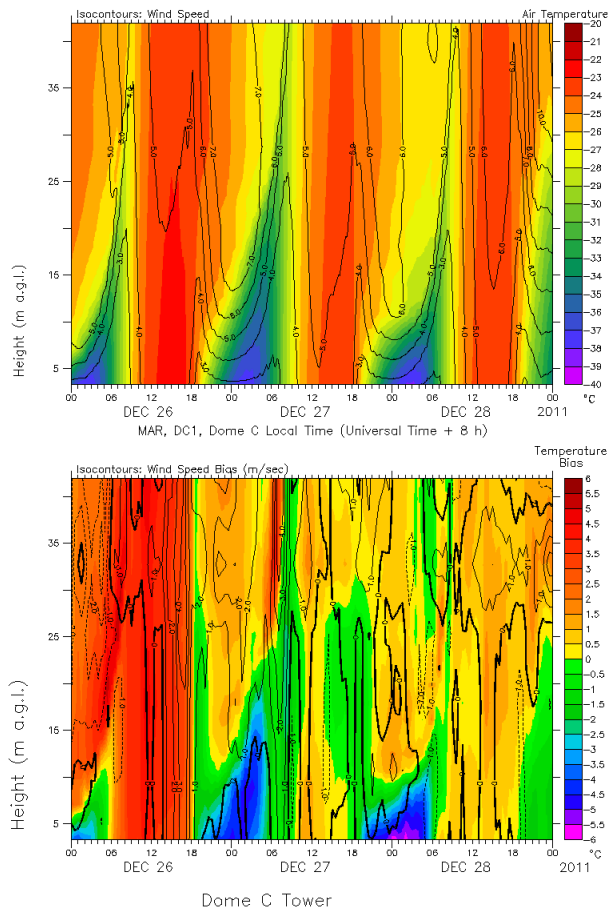


Figure 4. Temperature (color) and wind speed (isocontours) at the Dome C tower, as a function of LT (UT + 8 h) and height above the surface. **(a)** refers to MAR simulation (top), **(b)** to simulation minus observation (bottom).

Boundary layer at
Dome C during
summer

H. Gallée et al.

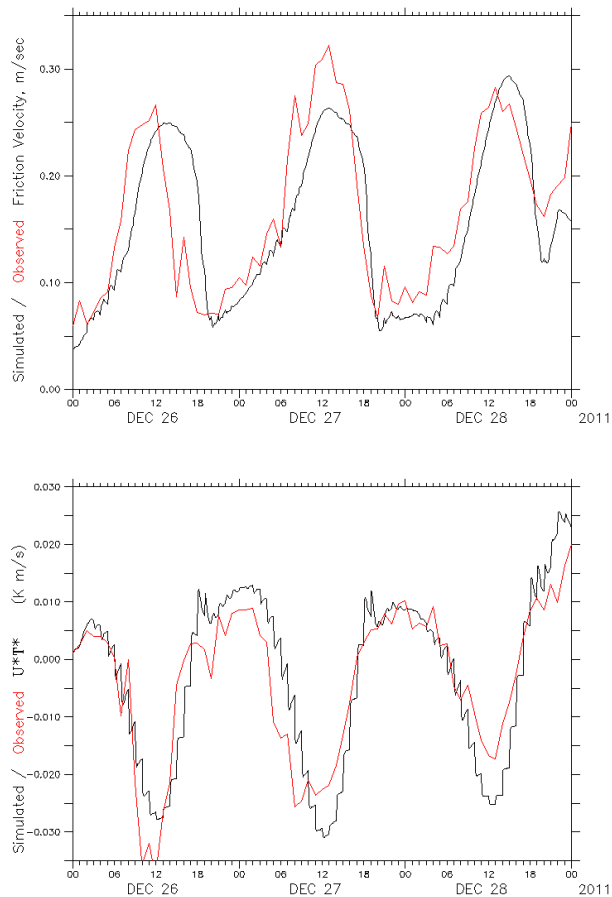


Figure 5. Surface turbulent fluxes at the Dome C tower, as a function of LT (UT + 8 h). **(a)** refers to the friction velocity (top), **(b)** to the sensible heat flux u^*T^* (bottom). The dark line is the MAR simulation, the red line the ISAC observations.

[Title Page](#)[Abstract](#)[Introduction](#)[Conclusions](#)[References](#)[Tables](#)[Figures](#)[Back](#)[Close](#)[Full Screen / Esc](#)[Printer-friendly Version](#)[Interactive Discussion](#)

